

Brain Tumor Classification using Deep Learning Models under Neutrosophic Environment

Ahmed Tolba ^{1*} , and Nourhan Talal ¹ 

¹ Department of Computer Science, Faculty of Computer and Informatics, Zagazig University, Zagazig, 44519, Egypt;
Emails: a.tolba24@fci.zu.edu.eg; N.Talal22@fci.zu.edu.eg.

* Correspondence: a.tolba24@fci.zu.edu.eg.

Abstract: A brain tumor is a highly malignant disease that affects both children and adults. Magnetic resonance imaging (MRI) is the most effective way to detect brain cancer. Scanning generates a huge amount of image data. This paper presents a study on the importance of neutrosophic sets (NS) in deep learning (DL) models for accurately classifying images. The work employs the NS and theory to convert medical images from the grayscale spatial domain to the neutrosophic domain. The purpose of this study is to investigate the effect of NS on DL models. The proposed work was evaluated on 3263 images of the brain tumor MRI dataset. The dataset is divided into four categories: glioma, meningioma, no tumor, and pituitary tumor. The study suggests that including the NS in DL models improves testing accuracy, especially when working with limited brain tumor datasets.

Keywords: Brain Tumors Classification, Neutrosophic Set, Deep Learning, Magnetic Resonance Imaging.

1. Introduction

Studies on brain tumors are currently highly popular within the academic community. Typically, cancer tumor classification involves dividing tumor regions into segments and categorizing the tumor [1, 2]. The central nervous system houses this crucial organ. Hence, brain tumors give rise to life-threatening conditions, making early detection crucial. The selection of features for brain tumor classification is crucial in determining the tumor's class membership. Magnetic Resonance Imaging (MRI) is employed to obtain crucial data regarding the morphology, dimensions, spatial orientation, and metabolic activity of brain tumors, thereby aiding in their diagnosis. Although a combination of modalities is used to obtain the most detailed information about brain tumors, MRI is considered the standard technique due to its excellent soft tissue contrast and widespread availability. MRI is a non-invasive imaging technique that uses radio frequency signals to stimulate target tissues and create internal images using a strong magnetic field. Various MRI sequences are produced by modifying excitation and repetition times during the process of image acquisition. Various MRI modalities yield distinct types of tissue contrast images [3].

Neutrosophic set (NS), an approach pioneered by Florentine Smarandache [4], is a robust technique that has gained significant popularity in recent times. Neutrosophy is founded upon the principles of neutrosophic logic, neutrosophic probability, NS theory, and neutrosophic statistics. The neutrosophic theory examines the source, characteristics, and extent of neutralities through the concept of a NS. It can also be linked to other fields of study. Within the framework of NS theory, situations are categorized and examined based on three distinct classifications: "True", "False", and "Indeterminacy". Due to its effectiveness in resolving indeterminacy issues, NS has been increasingly employed in image processing applications, including segmentation, edge detection, and thresholding. This is particularly relevant, as images often contain situations that are indeterminate.

NS have a crucial impact on image classification because they are highly effective in dealing with uncertainty, indeterminacy, and inconsistency. Managing Ambiguity Images frequently exhibit ambiguous or uncertain information as a result of noise, occlusion, or other contributing factors. NS enables the representation of uncertainty by assigning membership values to the set, as well as its indeterminacy and non-membership aspects. This enables classifiers to more accurately consider ambiguous areas within images. The significance of NS in image classification lies in their capacity to offer a resilient, adaptable, and efficient structure for managing the inherent uncertainties and complexities found in real-world image data.

DL techniques, particularly Convolutional Neural Networks (CNNs), have gained popularity among researchers due to their recent successes in various object recognition and biological image segmentation tasks [3].

Integrating NS with DL models in image classification provides an approach that combines the powerful capabilities of DL with the ability of NS to effectively deal with uncertainty, inconsistency, and ambiguity. This integration results in more robust, interpretable, and reliable classification systems. Overfitting is a common problem for DL models[5] particularly when they are trained on a small amount of data or data that contains noise. NS can enhance the resilience of DL models by allowing them to capture and represent uncertainty, thus reducing the chance of overfitting and improving performance. Also, interpreting decisions made by DL models can be difficult, especially in crucial domains such as medical diagnosis. NS [6] offer a clearer framework by explicitly representing uncertainty, indeterminacy, and non-membership, which can help improve understanding of classification results.

Three DL models are investigated in this study: ResNet50, MobileNet, and AlexNet. This paper proposes a novel NS based on DL models. Therefore, the incorporation of the NS into DL models may result in increased testing accuracy, especially when limited Brain Tumor datasets are used.

The primary contributions of the current investigation can be briefly summarized as follows:

- i. To eliminate the need for manual feature extraction, DL models are employed as a feature extractor.
- ii. For the first time, image processing with Neutrosophy was done using DL models.
- iii. A novel hybrid approach that combines classification and feature extraction.
- iv. Compared to traditional DL models, the classification performance of brain tumor images using NS and DL models was better.

The remainder of the paper is divided as follows. Section 2 presents the related work. Section 3 presents preliminaries for Neutrosophic theory and DL techniques. Section 4 presents the steps of the proposed approach. Section 5 presents experimental results. Section 6 describes managerial implications. Section 7 illustrates the conclusion and future directions of this proposal.

2. Related Work

Recently, researchers have become interested in unsupervised approaches due to their exceptional performance and the ability to automatically generate features, resulting in a reduction in error rates. DL models have become crucial in medical image analysis, including tasks like reconstruction, segmentation, and classification. Abhishta Bhandari et al. [7] suggested an automated segmentation model for the identification and separation of brain tumors using MRI brain images. CNNs are machine learning algorithms that are based on the biological processes of neurons (nodes) and synapses (connections). These algorithms have generated significant interest in the field.

The researchers examine the role of CNNs in classifying brain tumors. They begin by studying CNNs in an educational manner and conducting a literature search to establish a sample pipeline for classification. Next, they explore the future by employing CNNs to analyze a new domain called radionics. This analysis examines measurable characteristics of brain tumors, such as signal intensity,

shape, and texture, in order to predict clinical outcomes, including response to treatment and survival. Fatih Özyurt et al. [8] The study introduced a hybrid model that utilized a neutrosophy co-evolution neural network (NS-CNN). The goal is to categorize the region of the tumor in brain images as either benign or malignant. The initial phase involved segmenting MRI images using the NS-EMFSE method, which is based on the neutrosophy set and expert maximum fuzzy-sure entropy. The researchers acquired CNN and employed support vector machine (SVM) and k-nearest neighbors (KNN) classifiers to categorize the segmented brain images during the classification phase. The model was evaluated using 5-fold cross-validation on a dataset consisting of 80 benign tumors and 80 malignant tumors. The model's outcome demonstrates that the CNN features exhibited exceptional performance when utilized with various classifiers.

Pim Moeskops et al. [9] presented an automated model that uses a CNNs to classify MR brain images. They used different convolution kernel sizes and patch sizes to obtain multi-scale information about each voxel. Rather than depending on explicit features, the method uses training data to identify the key information needed for classification. To validate the model, their methodology necessitates using a single anatomical MR image. Five distinct datasets are used in this validation process.

Jamshid Sourati et al. [10] proposed a pioneering active learning technique utilizing Fisher information (FI) specifically designed for CNNs. By utilizing the efficient back propagation method to calculate gradients and employing a novel low-dimensional approximation of Fisher Information (FI), we were able to effectively compute FI for CNNs with a substantial number of parameters. The researchers assessed the suggested method for brain extraction. Using a patch-wise segmentation CNN model, we explore two distinct learning approaches: universal active learning and active semi-automatic segmentation. Two scenarios involved the creation of a starting model using the labeled training subjects from a dataset. The goal was to annotate a limited number of new samples in order to construct a model that accurately accomplishes the desired subject(s). The dataset consists of MR images that varied from the source data in terms of age, such as newborns with varying image contrast. The FI-based AL model demonstrated exceptional performance. Benjamin Thyreau et al. [11] This study presents an enhanced method for segmenting regions of the cerebral cortex in MRI brain images by utilizing ConvNets. A machine learning approach that efficiently applies the insights gained from surface analyses to more easily interpretable volume data. A ConvNets model is trained on a large dataset. A double MRI cohort's cortical ribbons dataset is used to replicate the parcellation obtained from a surface approach. In order to increase the applicability of the model in a wider range of situations, they compelled the model to adapt to segmentations that it had not previously encountered. The model is trained using data from cohorts that have not been previously observed. They provided a description of the approach's behavior while it was in the process of learning. The credence of the database itself was quantified, relying on the provision of a large training database, augmentation, and double contrasts. The ConvNets approach offers a highly effective and precise technique for rapidly segmenting MRI images.

Muhammad Attique Khan et al. [12] Suggested an automated DL approach for classifying brain tumors using multiple models. Their proposed model consisted of five phases. Initially, they utilized linear contrast stretching, which is based on edge histogram equalization and discrete cosine transform (DCT). Furthermore, they executed Feature extraction using DL. The process of transfer learning involved utilizing two pre-trained CNNs models, specifically VGG16 and VGG19, to extract features. Furthermore, they employed a correntropy-based joint learning approach utilizing the extreme learning machine (ELM) to leverage its most optimal selected features. In addition, they consolidated the strong covariant characteristics into a single matrix using the partial least squares (PLS) method for classification. The resulting matrix was then inputted into the ELM. Their proposed model was validated using the BRATS database and achieved a highest accuracy of 97.8%.

XinyuZhou et al. [13] Presented a novel approach for segmenting brain tumors by utilizing an efficient 3D residual neural network (ERV-Net) that minimizes GPU memory usage and computational complexity. Given the computational efficiency of the ERV-Net. The used ShuffleNetV2 is an encoder designed to enhance the efficiency of ERV-Net and minimize GPU memory usage. To prevent degradation, the decoder is equipped with residual blocks, also known as Res-decoder. To address the challenges of network convergence and data imbalance, the researchers enhanced a fusion loss function that combines dice loss and cross-entropy loss. Subsequently, they proposed a succinct and resilient pre-post methodology to enhance the preliminary segmentation output of ERV-Net. In order to assess the effectiveness of their model, the researchers utilized the dataset from the BRATS 2018, a challenge focused on segmenting brain tumors using multiple modalities. ERV-Net demonstrated superior performance, achieving dice scores of 81.8%, 91.21%, and 86.62%, as well as Hausdorff distances of 2.70 mm, 3.88 mm, and 6.79 mm for enhancing tumors. Another study [14] Introduced a novel neural network architecture called MBANet, which utilizes 3D convolution and 3D multi-branch attention. Initially, the optimized shuffle unit is employed to construct the fundamental unit (BU) module of MBANet. The BU module utilizes group convolution to execute the convolution operation following the division of the input channel. Additionally, it employs channel shuffle to reorganize the convolutional channels after fusion. The attention layer in the encoder of MBANet is a special multi-branch 3D Shuffle Attention (SA) module. The 3D SA module clusters the feature maps into smaller features by grouping them along the channel dimension. The 3D SA module incorporates both channel attention and spatial attention for each small feature, utilizing the BU module. Furthermore, to enhance the restoration of the upsampling semantic features, the skip connection of MBANet incorporates a 3D SA module. The experiments conducted on the BraTS 2018 and BraTS 2019 datasets demonstrate that the dice coefficients for the ET, WT, and TC regions are 80.18%, 89.80%, and 85.47%, respectively, for the first dataset, and 78.21%, 89.79%, and 83.04%, respectively, for the second dataset.

3. Materials and Methods

3.1 Preliminaries for Neutrosophic Theory

The NS can handle fuzziness and uncertainty in any data by using three membership sets to describe the attribute such as the *True (T)*, *Indeterminate(I)*, and *False (F)* subsets. a pixel P in the image is defined as $P(T, I, F)$ where T , I , and f are the true, indeterminate, and false in the set, respectively. Then, the pixel $P(a,b)$ in the image space is transformed into the NS space $PNS(a, b) = \{T(a, b), I(a, b), F(a, b)\}$. $T(a, b)$, $I(a, b)$ and $F(a, b)$ are the corresponding probabilities which are given by [15] :

$$T(a, b) = \frac{\bar{g}(a, b) - \bar{g}_{min}}{\bar{g}_{max} - \bar{g}_{min}} \quad (1)$$

$$\bar{g}(a, b) = \left(\frac{1}{w \times w} \right) \sum_{x=i-\frac{w}{2}}^{i+\frac{w}{2}} \sum_{y=a-\frac{w}{2}}^{a+\frac{w}{2}} g(x, y) \quad (2)$$

$$F(a, b) = 1 - T(a, b) \quad (3)$$

$$\delta(a, b) = abs(g(a, b) - \bar{g}(a, b)) \quad (4)$$

$$I(a, b) = \frac{\delta(a, b) - \delta_{min}}{\delta_{max} - \delta_{min}} \quad (5)$$

Where the local mean of the pixels in the window is $\bar{g}(a, b)$ and the absolute value of the difference between the intensity $g(a, b)$ and its $\bar{g}(a, b)$ is implied by $\delta(a, b)$.

The distribution of grey levels in an image can be ascertained using its entropy. The intensities have equal probability when the entropy is at its maximum. The distribution of intensity is not uniform if the entropy is low. An image's neutrosophic entropy is equal to the sum of its three subsets' entropies: I, T, and F [15]. The entropy can be calculated by the following:

$$Entropy_{NS} = Entropy_T + Entropy_I + Entropy_F \tag{6}$$

$$Entropy_T = - \sum_{j=\min\{T\}}^{\max\{T\}} P_T(Z) \ln P_T(Z) \tag{7}$$

$$Entropy_I = - \sum_{j=\min\{I\}}^{\max\{I\}} P_I(Z) \ln P_I(Z) \tag{8}$$

$$Entropy_F = - \sum_{j=\min\{F\}} P_F(Z) \ln P_F(Z) \tag{9}$$

Where the entropies are $Entropy_T$, $Entropy_I$, and $Entropy_F$ for T, I, and F, respectively. Furthermore, the probabilities of the element Z are $P_T(Z)$, $P_I(Z)$, and $P_F(Z)$ in T, I, and F, respectively.

3.2 Preliminaries on DL Models

This study examines three lightweight DL models: ResNet50, MobileNet, and AlexNet.

3.2.1 ResNet50 Model

The architecture of ResNet50 model [1] displays in Figure 1. The Modified ResNet50 Model is created by removing the last layer of the ResNet50 and adding the smooth, thick, dropout, and dropout layers as additional layers. The sigmoid function is then used because it can translate the output of the model into a probability value, which is easier to manipulate and understand.

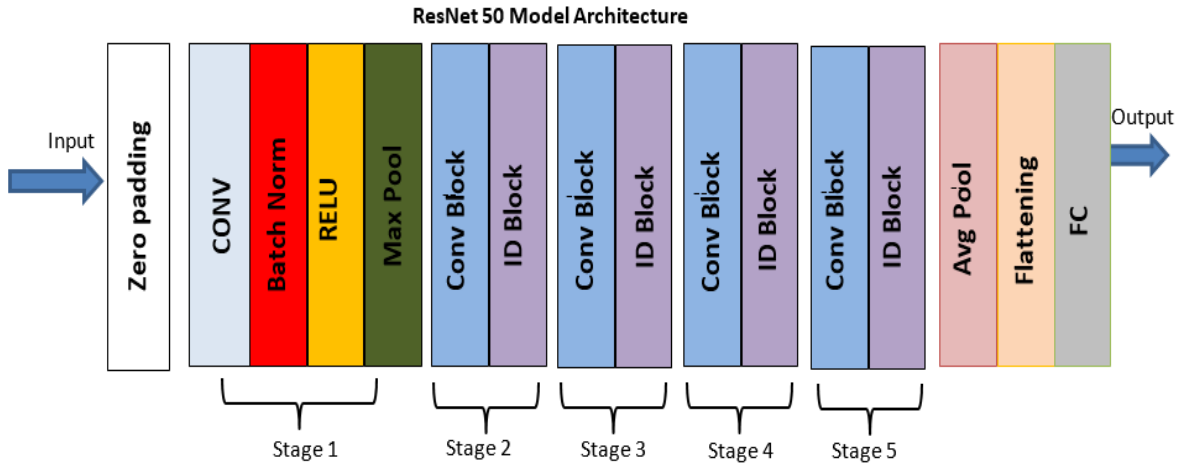


Figure 1. ResNet 50 model architecture [1].

This would translate mathematically to $y = x + F(x)$, where y is the layer's final output. Figure 2 shows the residual block in ResNet50.

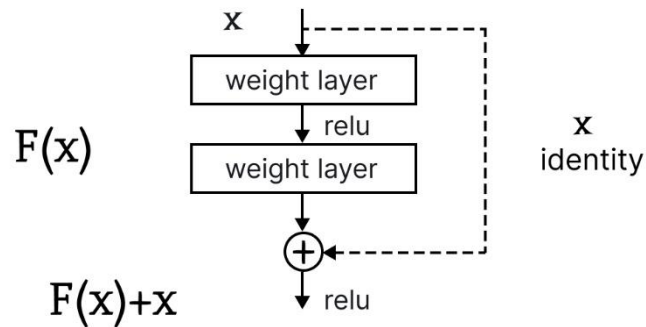


Figure 2. Residual learning, building block [1].

3.2.2 MobileNet Model

One CNN architecture called MobileNet can do away with the requirement for excessive computer power[16]. Convolution is split into depthwise and pointwise subtraction by MobileNet. Batch Normalization BN and Rectified-Linear units ReLU are used by the MobileNet architecture for depthwise and pointwise convolution, respectively [17].

Generally, the main distinction between the MobileNet architecture and the CNN architecture lies in the utilization of a convolution layer or layer with a filter thickness that matches the thickness of the input image. MobileNet employs a division of convolution into two separate operations: depthwise convolution and pointwise convolution, as illustrated in Figure 3 and Figure 4 [18, 19]. Figure 4 depicts the Left side Standard convolutional layer with batch normalization and Rectified Linear Unit (ReLU). In addition, the site employs Depthwise Separable convolutions, which consist of Depthwise and Pointwise layers, followed by batch normalization and Rectified Linear Unit (ReLU) activation.

MobileNet's structure consists of deep, separable convolutions, with the exception of the first layer, which is full convolution. Defining the network in simple terms allows for easy exploration of topology to improve the network.

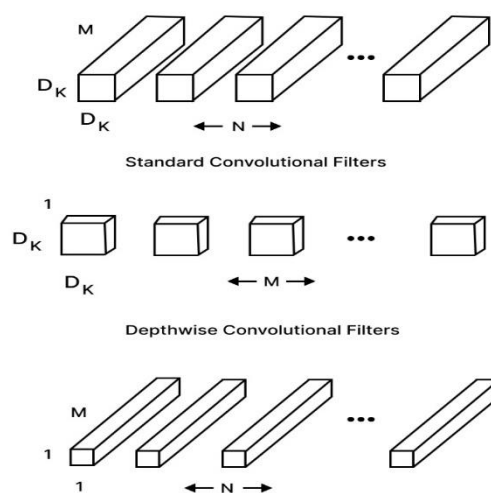


Figure 3. Convolution standard.

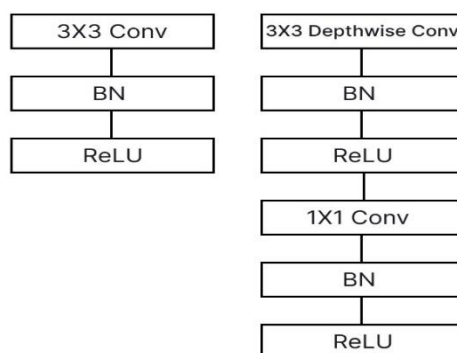


Figure 4. Convolution layer.

3.2.3 AlexNet Model

AlexNet [20, 21] is used in this study for extraction due to its exceptional accuracy on testing datasets. AlexNet is the most well-known deep CNN structure, with 25 layers, eight of which enhance learning by modifying loads. Five of these layers are convolutional, while the remaining three are fully connected (FC). The AlexNet design connects max-pooling layers to convolution layers in series. The initial convolution layer and subsequent max-pooling layers make use of varying kernel sizes [22]. The layer of max-pooling follows the layer of convolution [22]. The first FC layer, FC6, and the second FC layer, FC7, are used to remove vector features during activation. The AlexNet CNN design includes 4096 features for FC6 and FC7 vectors [23].

4. Proposed Approach

The research methodology involves proposing a model capable of accurately classifying brain tumor diseases using MRI images into four distinct categories. The proposed model consists of two primary components: the first component is neutrosophic domain conversion, and the second component is the transfer learning architectures. Figure 6 depicts the proposed neutrosophic/DTL model for the study. The neutrosophic image domain conversion is employed as a preliminary step in the process, while the DTL structures are utilized throughout the training and testing stages.

4.1 Neutrosophic Image Domain Conversion

Neutrosophic image domain conversion is the process of converting conventional images into a representation in the neutrosophic domain. Neutrosophy, a concept introduced by Florentin Smarandache, In the theory of NS, events are analyzed by dividing them into three subsets: the True (T) neutrosophic domain, the Indeterminacy (I) neutrosophic domain, and the Falsity (F) neutrosophic domain. The pixels in the correct subset correspond to specific or dependable data, whereas the pixels in the false subset correspond to uncertain or unreliable data. The indeterminate subset encompasses information that is uncertain, vague, or contradictory. The NS theory is a valuable and beneficial concept in the field of computing for dealing with ambiguous situations. Neutrosophic domain conversion in image processing seeks to capture and express the inherent uncertain or ambiguous information found in images. For tasks like object and edge detection, the pixels of the image are separated into three subsets: T, I, and F. Next, the image performs edge detection and object processing using essential operations on these subsets. The input image is transformed into the neutrosophic domain, as demonstrated by Equations (1-5).

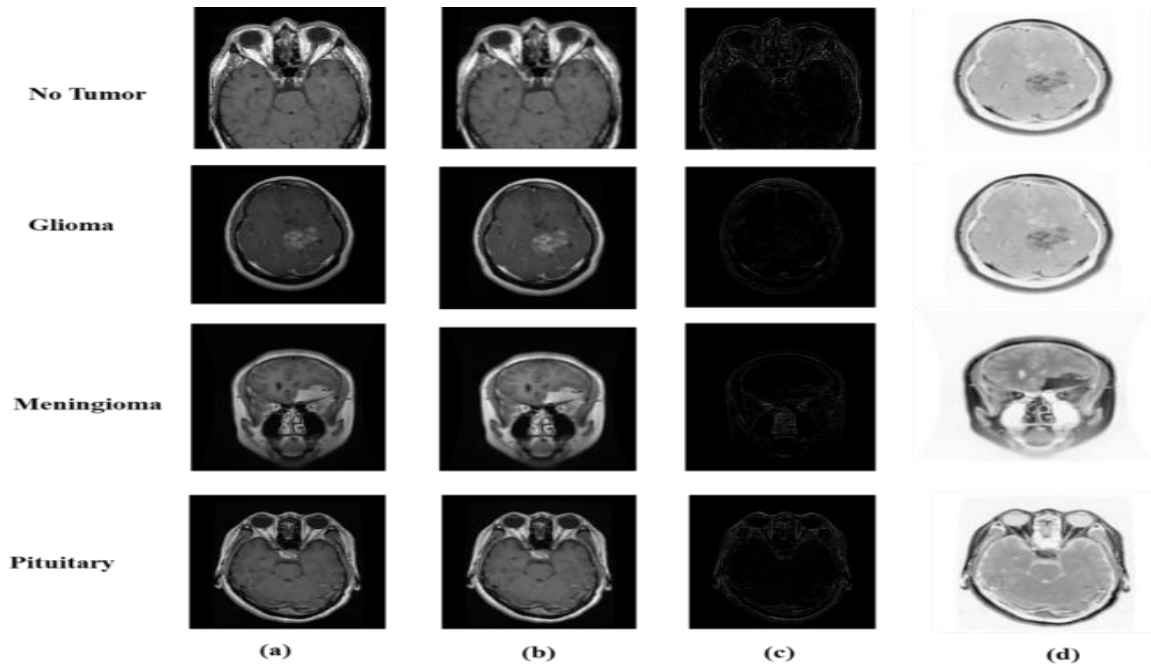


Figure 5. Different neutrosophic images domain for 4 labels from brain were (a) original images, (b) True neutrosophic domain, (c) Indeterminacy neutrosophic domain, and (d) Falsity neutrosophic domain image.

4.2 Deep Learning Transfer Learning Architectures

Deep transfer learning models using a different images domain of brain tumor dataset [1]

- The Original dataset domain (grayscale).
- The True (T) neutrosophic domain.
- The Indeterminacy (I) neutrosophic domain.
- The Falsity (F) neutrosophic domain.

The process flow of the deep transfer learning models starts by extract significant features from a preprocessed dataset of brain tumor diseases. Next, the training dataset is partitioned into different sets for training and validation by 90% and 10 %, respectively. The training dataset is employed for the purpose of training DL model. The validation dataset is utilized to evaluate the performance of the model and make improvements to its parameters. Lastly, the testing dataset is applied to examine the final performance and generalization capabilities of the trained model on unknown data. Compared to several DL models, such as ResNet50, AlexNet and MobileNet. Those models are chosen based on their architecture, which feature a limited number of layers. To evaluate the efficiency of the conversion process to the neutrosophic domain, all models are implemented in Python using the Kaggle platform and keras API. Regarding the loss function, the all models compiled with the categorical cross-entropy loss, Categorical cross-entropy is a loss function often used in classification tasks involving several classes. It evaluates the dissimilarity between predicted values probabilities and the true values labels. The goal is to minimize this dissimilarity during training, helping the model learn to effectively classify new data into the correct categories.

$$\text{Minimize: loss} = - \sum_{i=1}^M y_i \cdot \log \check{y}_i \quad (10)$$

Where y_i represent real values and \check{y}_i represent predicted values.

The Adam optimizer was used to train the weights of those models for 30 epochs with batch size 32. In addition, the early stopping with a patience of 5 was used in our experiments. Where it plays an essential role in reducing training time and computational complexity. Where the training method will commence at a certain location. If there is no improvement in the validation accuracy for 5 epochs the weights of the network will be stopped.

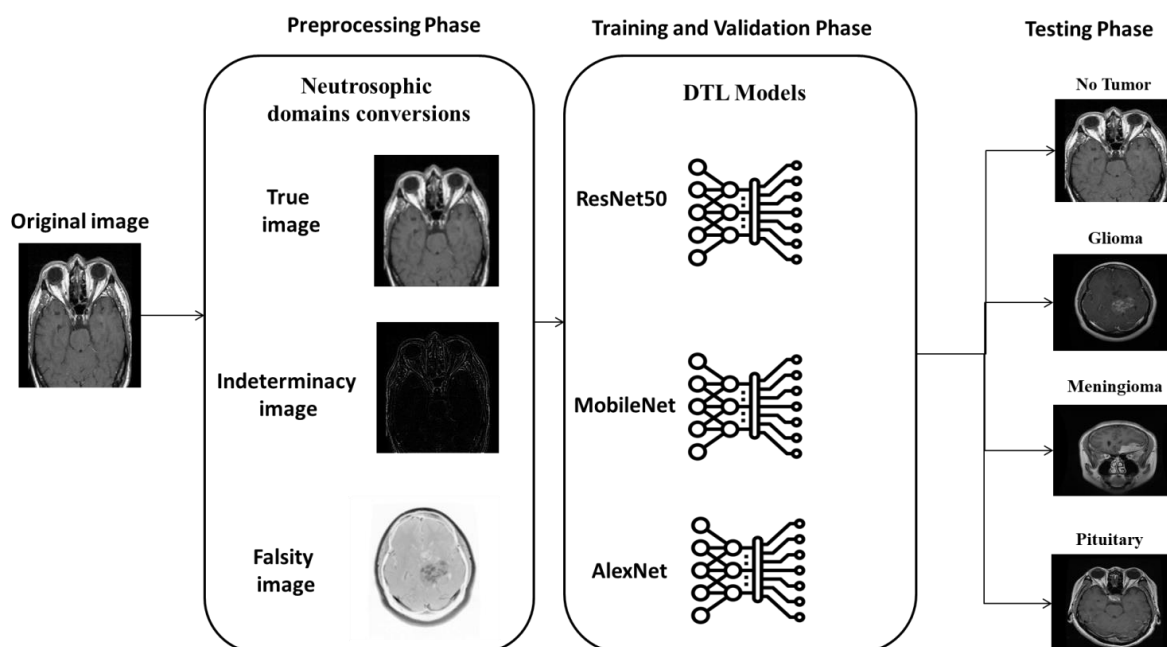


Figure 6. Proposed neutrosophic/DTL model for this study.

5. Experimental Results

This part includes the MRI image dataset overview, evaluation metrics, statistical, and computational complexity analysis related to tumor image classification.

5.1 Dataset Description

The Brain Tumor dataset [24] was adjusted to a resolution of 512×512 pixels and had a total of 3263 categorized images brain tumor diseases. The dataset split into two part the first part is training data that contains 2870 images and the second part is testing data that contains a 393 of brain tumor diseases each part classified into 4 labels, with 3 corresponding to diseases and one corresponding to health. Figure 7 describe Depiction of infected and healthy images in this dataset. The dataset is categorized into four classes: glioma_tumor, meningioma_tumor, non_tumor, and pituitary_tumor. Table 1 clearly describes the distribution of each class in this dataset. Finally, before starting the training process, the images in this dataset are first resized to 150×150 pixels.

Table 1. Description of used brain tumor dataset.

Classes	glioma_tumor	meningioma_tumor	no_tumor	pituitary_tumor
Training	826	822	395	827
Testing	100	115	105	73

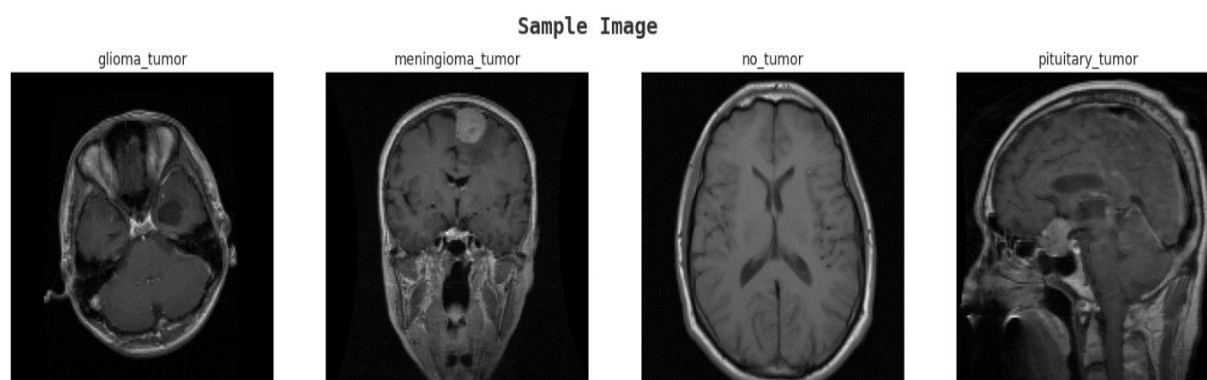


Figure 7. Depiction of infected and healthy images in this dataset.

5.2 Performance Evaluation Metrics

$$\text{Accuracy} = \frac{TP+TN}{TP+FP+TN+FN} \quad (2)$$

$$\text{Precision} = \frac{TP}{TP+FP} \quad (3)$$

$$\text{Recall} = \frac{TP}{TP+FN} \quad (4)$$

$$\text{F1 - score} = 2 * \frac{\text{Precision} \cdot \text{Recall}}{\text{Precision} + \text{Recal}} \quad (5)$$

$$\text{AUC} = \frac{1 + \frac{TP}{TP+TN} \frac{FP}{FP+TN}}{2} \quad (6)$$

Where TP, FN, TN, and FP represent the number of true positive, the number of false negative, the number of true negative, and the number false positive, respectively.

- **Accuracy:** The ratio of accurately predicted samples to the total number of samples.
- **Precision:** The ratio of accurately identified positive instances to the total number of predicted positive instances.
- **Recall:** Is a metric that estimates the model's capacity to accurately detect positive instances among all the actual positive samples.
- **F1-score:** is the harmonic mean of precision and recall.
- **AUC:** It represents the model's ability to distinguish between positive and negative instances, with a higher AUC indicating better performance.
- **Confusion Matrix:** It is a method of presenting the count of correct and incorrect instances according to the model's predictions.

5.3 Statistical Analysis

This section investigates the performance of the Deep transfer learning under neutrosophic domain.

5.3.1 MRI image Classification using DL Model Statistical Analysis

Table 2 presents the testing accuracy and performance metrics for DTL models with original dataset the table clearly shows that the Resnet50 model achieves the highest accuracy and AUC with 73.8% and 81.6 % with close scores in performance metrics. Followed directly by the MobileNetV2 model where it achieves accuracy and AUC with 72.0% and 80.4 %.

Table 2. Testing accuracy and performance metrics for DTL models with original dataset.

Model	Accuracy	Precision	Recall	F1-Score	AUC
ResNet50	0.738	0.826	0.724	0.706	0.816
MobileNet	0.720	0.808	0.705	0.670	0.804
AlexNet	0.576	0.720	0.562	0.545	0.708

5.3.2 MRI image Classification using DL Model under neutrosophic domain statistical analysis

The neutrosophic domains consist of three distinct types: the True (T) neutrosophic domain, the Indeterminacy (I) neutrosophic domain, and the Falsity (F) neutrosophic domain. The performance of those neutrosophic domains will be examined in this section.

The first neutrosophic domain for experimentation is the True (T) neutrosophic domain. "Neutrosophic Image Domain Conversion" refers to the process of transforming an original image into a True (T) image by averaging each pixel with its neighboring pixels within a chosen window. The window size chosen for this study is 5 pixels. The Falsity (F) neutrosophic domain is the second domain being tested. This domain is the antithesis of the True (T) neutrosophic domain. In the Falsity (F) domain, the values of all pixels are reversed, resulting in the hiding of certain features and the exposure of other aspects in images. The Indeterminacy (I) neutrosophic domain is the third domain to undergo experimentation. This domain encompasses the farthest boundaries inside the image. In the Indeterminacy (I) domain, each pixel value is obtained by subtracting the original pixel value from the average pixel value in the True (T) neutrosophic domain. Table 3 displays the Testing accuracy and performance metrics for DTL models for the True domain (T), Falsity domain (F) and Indeterminacy (I) domain.

Table 3. Testing accuracy and performance metrics for DTL models for the True domain (T), Falsity domain (F) and Indeterminacy (I) domain.

Domain	Model	Accuracy	Precision	Recall	F1-Score	AUC
True image	ResNet50	0.746	0.837	0.737	0.711	0.824
	MobileNet	0.720	0.742	0.718	0.675	0.811
	AlexNet	0.634	0.708	0.633	0.590	0.754
False image	ResNet50	0.756	0.815	0.739	0.722	0.827
	MobileNet	0.710	0.788	0.686	0.659	0.793
	AlexNet	0.329	0.377	0.366	0.258	0.575
Indeterminacy image	ResNet50	0.741	0.777	0.727	0.702	0.819
	MobileNet	0.741	0.810	0.731	0.699	0.820
	AlexNet	0.637	0.631	0.634	0.621	0.755

Table 3 illustrates that in the True (T) neutrosophic domain and Falsity (F) neutrosophic domain, both ResNet50 and MobileNetV2 models achieve highest testing accuracy with 74.6 % and 72.0 % in T domain and 75.6 % and 71.0 % in F domain, with an advantage for the ResNet50 model in the achieved performance metrics. In the Indeterminacy (I) neutrosophic domain both ResNet50 and MobileNetV2 models achieve similar highest testing accuracy with 74.1% with an advantage for the MobileNet model in the achieved performance metrics.

5.4 Visual Analysis

Confusion matrix for the best model that obtained results in the neutrosophic domain compared to the original data. Figures 8, 9, and 10 display confusion matrices that represent the classification

performance of two separate models. ResNet50 is implemented using the Falsity (F) neutrosophic domain and the original data. MobileNet is implemented using the Indeterminacy (I) neutrosophic domain and the original data. AlexNet is implemented using the True (T) neutrosophic domain and the original data. The use of the neutrosophic domain clearly has a significant influence on the classification accuracy and resilience of the model. Upon examining the confusion matrix of each model using the neutrosophic domain, it is evident that there are significantly higher values along the diagonal elements. This suggests that there is a larger number of examples correctly classified for each class. In contrast, the off-diagonal elements, which indicate misclassifications, had significantly lower frequencies as compared to the confusion matrix of models using the original data. The difference in performance indicates that the neutrosophic domain model achieves higher accuracy in classification and shows fewer cases of misclassification.

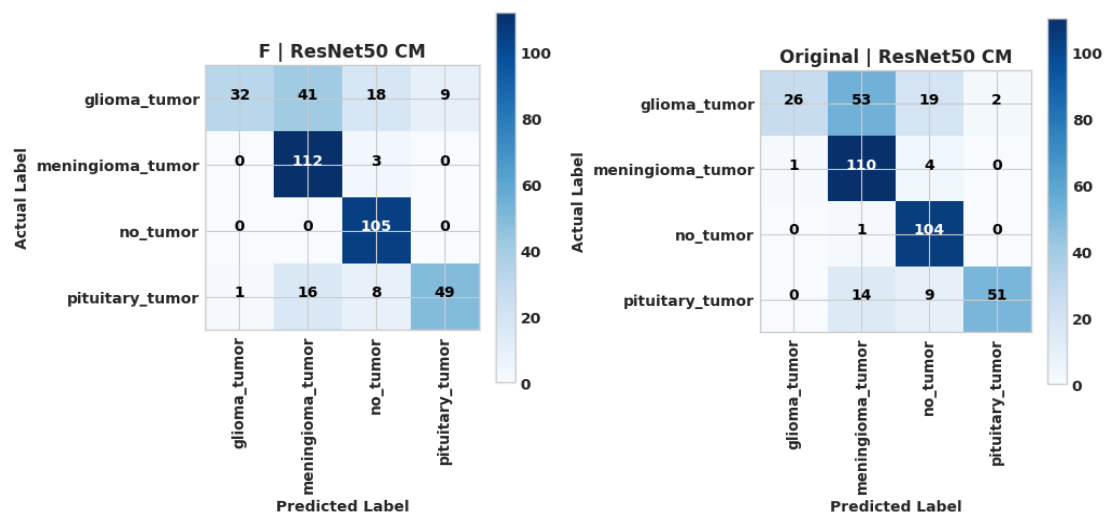


Figure 8. Confusion matrix of the ResNet50 model in the original dataset and Falsity (F) neutrosophic domain.

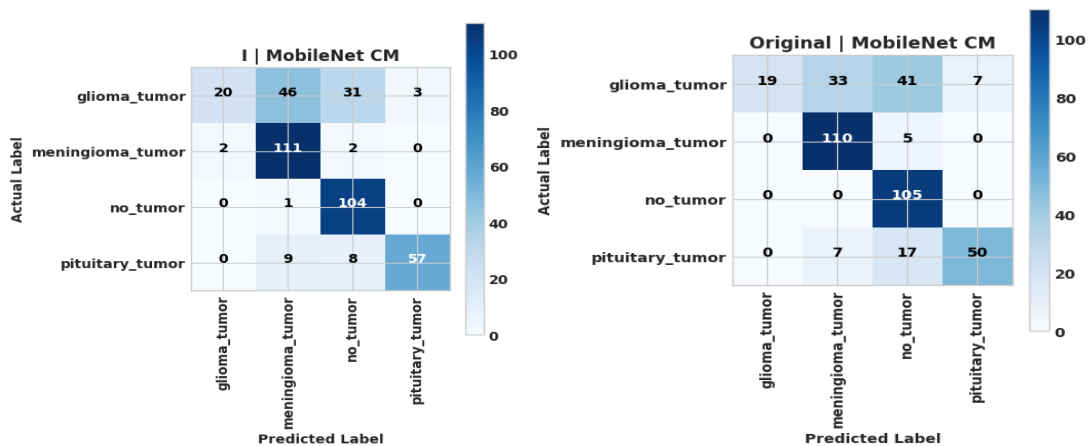


Figure 9. Confusion matrix of the MobileNet model in the original dataset and Indeterminacy (I) neutrosophic domain.

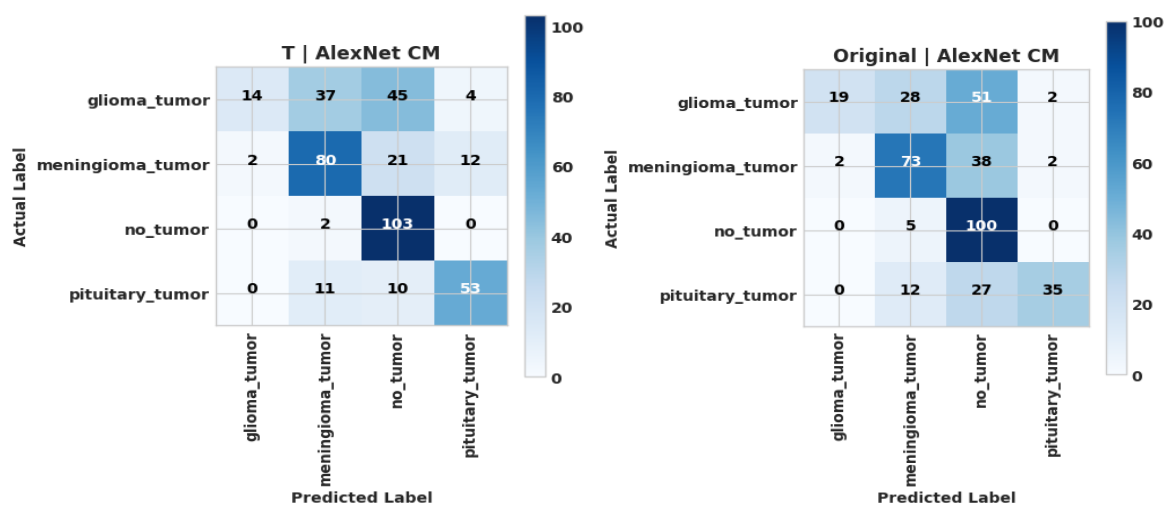


Figure 10. Confusion matrix of the AlexNet model in the original dataset and True (T) neutrosophic domain .

6. Managerial Implications

To achieve sustainable healthcare development, Egypt must meet its Vision 2030 target. The advancement of machine learning and deep learning approaches for image analysis has the potential to transform brain tumor detection and therapy. Using AI in medical image detection and classification can improve healthcare services and increase accurate diagnoses. Furthermore, early and correct detection of brain tumors can lead to better treatment outcomes, fewer deaths, and a higher quality of life. It can also save time and money over standard diagnostic methods, making it more accessible to patients in remote or underserved areas. Technology can open up new career opportunities in the healthcare and technology sectors while also improving healthcare infrastructure. In this context our study proposed a integration between deep learning (DL) models and neutrosophic theory to classify MRI images. The use of NS and theory aims to handle more degrees of uncertainty by represent medical image into three subsets: true (T), indeterminacy (I), and false. ResNet50, MobileNet, and AlexNet were DL models selected for the image classification process. These models are chosen based on their designs, which are distinguished by a limited number of layers. According to the experimental results, the MobileNet with Indeterminacy (I) neutrosophic domain achieves the maximum testing accuracy of 74.2%. It also performs well in metrics like Precision, Recall, F1 Score, and AUC. The ResNet50 model, which employs the True (T) neutrosophic domain, achieves a maximum accuracy of 74.6% in both testing accuracy and other performance measures. Other performance metrics are best achieved by the AlexNet model, which is implemented with the True (T) neutrosophic domain. This research study can be used to effectively improve brain tumor image. So, the proposed work can offer and serve the healthcare sector to achieve Egypt vision 2030.

7. Conclusion and Future Work

In this study, given the scarcity of brain tumor datasets, combining DL models with the neutrosophic set could be a promising way to improve testing accuracy. Trying the proposed model on larger datasets is one of the possible future projects. Furthermore, incorporate deeper transfer learning into experimental research by combining models such as the X-ception model with neutrosophic theory.

This study proposes a novel and efficient method for extracting and categorizing features from brain MRIs to classify brain tumors. ResNet50, MobileNet, and AlexNet were chosen as the deep learning models for this study. We obtained 74.2%, 74.6% and achieved the highest other accuracy metrics using the MobileNet, ResNet50, and AlexNet models, respectively. However, the proposed model was evaluated using a dataset of 3263 images. Our approach is highly applicable in the health sector, where we offer innovative solutions with exceptional accuracy for medical imaging, particularly in the more precise diagnosis of brain tumors.

We intend to investigate how combining DL models and neutrosophic techniques with multimodal imaging data (e.g., MRI, CT, and PET) can improve classification precision and provide more comprehensive insights into the characteristics of brain tumors.

Funding

This research received no external funding.

Ethical approval

This research does not contain any studies with human participants or animals performed by any of the authors.

Conflicts of Interest

The authors declare that there is no conflict of interest in the research.

Institutional Review Board Statement

Not applicable.

Informed Consent Statement

Not applicable.

Data Availability Statement

Not applicable.

References

- [1] Sharma, A.K., et al., Brain tumor classification using the modified ResNet50 model based on transfer learning. *Biomedical Signal Processing and Control*, 2023. 86: p. 105299.
- [2] Ari, A. and D. Hanbay, Deep learning based brain tumor classification and detection system. *Turkish Journal of Electrical Engineering and Computer Sciences*, 2018. 26(5): p. 2275-2286.
- [3] Işın, A., C. Direkoğlu, and M. Şah, Review of MRI-based brain tumor image segmentation using deep learning methods. *Procedia Computer Science*, 2016. 102: p. 317-324.
- [4] Smarandache, F., A unifying field in logics: neutrosophic logic. *Neutrosophy, neutrosophic set, neutrosophic probability: neutrosophic logic*. Neutrosophy, neutrosophic set, neutrosophic probability. 2005.
- [5] Bhatt, C., et al., The state of the art of deep learning models in medical science and their challenges. *Multimedia Systems*, 2021. 27(4): p. 599-613.
- [6] Akbulut, Y., et al., NS-k-NN: Neutrosophic set-based k-nearest neighbors classifier. *Symmetry*, 2017. 9(9): p. 179.
- [7] Bhandari, A., J. Koppen, and M. Agzarian, Convolutional neural networks for brain tumour segmentation. *Insights into Imaging*, 2020. 11(1): p. 77.
- [8] Özyurt, F., et al., Brain tumor detection based on Convolutional Neural Network with neutrosophic expert maximum fuzzy sure entropy. *Measurement*, 2019. 147: p. 106830.
- [9] Moeskops, P., et al., Automatic segmentation of MR brain images with a convolutional neural network. *IEEE transactions on medical imaging*, 2016. 35(5): p. 1252-1261.
- [10] Sourati, J., et al., Intelligent labeling based on fisher information for medical image segmentation using deep learning. *IEEE transactions on medical imaging*, 2019. 38(11): p. 2642-2653.

- [11] Thyreau, B. and Y. Taki, Learning a cortical parcellation of the brain robust to the MRI segmentation with convolutional neural networks. *Medical image analysis*, 2020. 61: p. 101639.
- [12] Khan, M.A., et al., Multimodal brain tumor classification using deep learning and robust feature selection: A machine learning application for radiologists. *Diagnostics*, 2020. 10(8): p. 565.
- [13] Zhou, X., et al., ERV-Net: An efficient 3D residual neural network for brain tumor segmentation. *Expert Systems with Applications*, 2021. 170: p. 114566.
- [14] Cao, Y., et al., MBANet: A 3D convolutional neural network with multi-branch attention for brain tumor segmentation from MRI images. *Biomedical Signal Processing and Control*, 2023. 80: p. 104296.
- [15] Guo, Y., H. Cheng, and Y. Zhang, A new neutrosophic approach to image denoising. *New Mathematics and Natural Computation*, 2009. 5(03): p. 653-662.
- [16] Sae-Lim, W., W. Wettayaprasit, and P. Aiyarak. Convolutional neural networks using MobileNet for skin lesion classification. in *2019 16th international joint conference on computer science and software engineering (JCSSE)*. 2019. IEEE.
- [17] Pan, H., et al., A new image recognition and classification method combining transfer learning algorithm and mobilenet model for welding defects. *Ieee Access*, 2020. 8: p. 119951-119960.
- [18] Howard, A.G., et al., Mobilenets: Efficient convolutional neural networks for mobile vision applications. *arXiv preprint arXiv:1704.04861*, 2017.
- [19] Sinha, D. and M. El-Sharkawy. Thin mobilenet: An enhanced mobilenet architecture. in *2019 IEEE 10th annual ubiquitous computing, electronics & mobile communication conference (UEMCON)*. 2019. IEEE.
- [20] Ali, N.A., et al. Design of automated computer-aided classification of brain tumor using deep learning. in *Intelligent and Interactive Computing: Proceedings of IIC 2018*. 2019. Springer.
- [21] Krishnammal, P.M. and S.S. Raja. Convolutional neural network based image classification and detection of abnormalities in mri brain images. in *2019 International Conference on Communication and Signal Processing (ICCSP)*. 2019. IEEE.
- [22] Coşkun, M., et al., An overview of popular deep learning methods. *European Journal of Technique (EJT)*, 2017. 7(2): p. 165-176.
- [23] Simonyan, K. and A. Zisserman, Very deep convolutional networks for large-scale image recognition. *arXiv preprint arXiv:1409.1556*, 2014.
- [24] SARTAJ. Brain Tumor Classification (MRI). 2020; Available from: <https://www.kaggle.com/datasets/sartajbhuvaji/brain-tumor-classification-mri>.

Received: 01 Dec 2023, **Revised:** 18 Mar 2024,

Accepted: 17 Apr 2024, **Available online:** 21 Apr 2024.



© 2024 by the authors. Submitted for possible open access publication under the terms and conditions of the Creative Commons Attribution (CC BY) license (<http://creativecommons.org/licenses/by/4.0/>).

Disclaimer/Publisher's Note: The perspectives, opinions, and data shared in all publications are the sole responsibility of the individual authors and contributors, and do not necessarily reflect the views of Sciences Force or the editorial team. Sciences Force and the editorial team disclaim any liability for potential harm to individuals or property resulting from the ideas, methods, instructions, or products referenced in the content.